JOURNAL OF CHEMICAL INFORMATION AND MODELING

Article

pubs.acs.org/jcim

Molecular Docking Characterizes Substrate-Binding Sites and Efflux Modulation Mechanisms within P-Glycoprotein.

Ricardo J. Ferreira,[†] Maria-José U. Ferreira,[†] and Daniel J. V. A. dos Santos*[,†,‡]

[†]Research Institute for Medicines and Pharmaceutical Sciences (iMed.UL), Faculty of Pharmacy, University of Lisbon, Av. Prof. Gama Pinto, 1649-003 Lisbon, Portugal

[‡]REQUIMTE, Department of Chemistry & Biochemistry, Faculty of Sciences, University of Porto, Rua do Campo Alegre, 4169-007 Porto, Portugal

Supporting Information

ABSTRACT: P-Glycoprotein (Pgp) is one of the best characterized ABC transporters, often involved in the multidrug-resistance phenotype overexpressed by several cancer cell lines. Experimental studies contributed to important knowledge concerning substrate polyspecificity, efflux mechanism, and drug-binding sites. This information is, however, scattered through different perspectives, not existing a unifying model for the knowledge available for this transporter. Using a previously refined structure of murine Pgp, three putative drug-binding sites were hereby characterized by means of molecular docking. The modulator site (M-site) is characterized by cross interactions between both Pgp halves herein defined for the first time, having an important role in impairing conformational changes leading to substrate efflux. Two other binding sites, located next to the inner leaflet of the lipid bilayer, were identified as the substrate-binding H and R sites by matching docking and experimental results. A new classification model with the ability to discriminate substrates from modulators is also proposed, integrating a vast number of theoretical and experimental data.

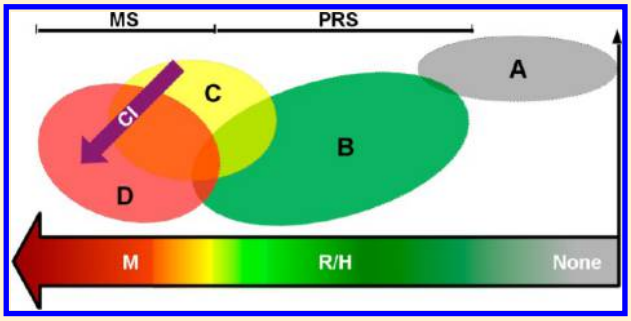

P-Glycoprotein (Pgp) is one of the ABC transporters more frequently implied in multidrug-resistance (MDR) phenomenon due to the ATP-driven increased efflux of many chemotherapeutic agents, which reduces intracellular concentrations and impairs their pharmacological effect. This transporter is characterized by a pseudo-2-fold molecular symmetry comprising two functional units, each with six transmembrane α-helices domains (TMDs) and one cytoplasmic nucleotide-binding domain (NBD) responsible for ATP binding and hydrolysis.[1]

The discovery of efflux modulation by verapamil was the starting point of further experimental studies,[2] aiming to a clarification of possible drug-binding sites (DBSs), translocation pathways, and intrinsic characteristics of the mechanism. These early studies quickly identified physicochemical characteristics (log$P$[3,4] and hydrogen-bond donor/acceptor atoms[5]) as important in substrate recognition, whereas aromatic moieties[6] and nitrogen atoms[3,7] appeared to be essential for the efflux modulation. Another approach was based on pharmacophore development,[7−10] in an attempt to identify not only the most suitable characteristics but also the optimal spatial arrangement needed for an effective Pgp modulation. Two efflux mechanisms were later proposed, the flippase[11] model and the membrane pore,[12] from which a third one, the most currently accepted "hydrophobic vacuum-cleaner" model, was further developed.[13]

However, several doubts remained about the drug-binding sites specific locations. In the later 1990s, Shapiro and Ling proposed the existence of two distinct DBSs, positively cooperating with each other, naming them the H-site and the R-site due to the distinct drug specificities registered for Hoechst 33342 and rhodamine-123, respectively.[14] According to the authors, Hoechst 33342, Hoechst 33258, quercetin, and colchicine would interact preferentially with the H-site and rhodamine-123, doxorubicin, daunorubicin, and other anthracyclines with the R-site. Moreover, it was also shown that molecules could be removed from the inner leaflet to the outer leaflet of the lipid bilayer through both sites,[15] supporting the vacuum-cleaner model and postulating the existence of two distinct translocation pathways (recently confirmed[16]). A later study, using matrix-assisted laser desorption/ionization time-of-flight (MALDI-TOF) mass spectrometry and photoaffinity ligands, located these sites in each of the halves of Pgp, next to the TMDs 3/11 and 5/8.[17] In the same year, another study identified residues in TMDs 4−6 and 9−12 as belonging to a common drug-binding pocket (DBP), identifying one possible drug-binding site (DBS) at the interface between TMDs 1 and 2.[18] A third drug-binding site was also proposed, with a positive allosteric effect on both H- and R-sites (probably by interfering with ATP-hydrolysis rate).[19] Sharom et al.,[20,21] by means of

Received: April 2, 2013
Published: June 26, 2013

dx.doi.org/10.1021/ci400195v | J. Chem. Inf. Model. 2013, 53, 1747−1760

fluorescence resonance energy transfer (FRET) studies, additionally mapped potential locations for H- and R-sites within the inner (cytoplasmic) leaflet of the lipid bilayer, suggesting a symmetrical structure functionally related, however not excluding a common central drug-binding site. The identification of such sites offered, for the first time, a plausible explanation for the polyspecificity of Pgp through the theorization of a 'substrate induced-fit' model in multidrug binding.[22] In addition, the identification of specific residues linked to substrate binding (protected from methanethiosulfonate− MTS− labeling by verapamil) allowed to precise the location, in human Pgp, at TMDs 4 (Ser222), 5 (Ile306), 6 (Leu339, Ala342), 10 (Ile868), 11 (Phe942, Thr945), and 12 (Gly984).

Further studies increased the pool of residues involved in drug-binding and located them at the interface of TMDs facing a hypothetical internal DBP. The majority of these residues are found in TMD 6 (Leu339, Ile340, Ala342, Phe343) and TMD 12 (Leu975, Val981, Val982, Gly984, Ala985),[23] suggesting that TMDs 2, 3, 5, and 7−11 are spatially organized to form a funnel-shaped drug-binding pocket.[24] More recently and in an attempt to map potential interaction sites, Mandal et al.[25] found evidence of two modulator-specific sites for Z-flupentixol at the human Pgp-lipid interface, demonstrating that residues Met948 (TMD11), Phe983, Met986, Val988, and Gln990 (TMD12) were involved in substrate-site modulation toward iodoarylazidoprazosin (^{125}IAAP). For ATPase activity modulation, four residues were identified— Thr837, Ile864, Met948, and Gln990— with the last two residues common to substrate modulation.

Despite important contributions by the described studies, none completely defined the specific location of H and R sites in the Pgp structure. However, all of the above studies suggest a central location within the internal cavity as a key area for Pgp modulation, locating this area between the two functional units at the same level of the outer membrane leaflet. H and R sites, probably located next to the inner interface of the lipid bilayer, still remain largely unknown and uncharacterized namely in its amino-acid composition, physicochemical characteristics or exact location in the internal DBP.

The publication of a tridimensional structure of hamster Pgp in the nucleotide-bound state (with approximately 8 Å resolution[26]) provided the first structural evidence for the existence of an internal DBP. Although similar to MsbA (*E. coli* Pgp homologue) with respect to the transmembranar helices packing, differences were found in the number of interactions responsible for the packing of the two halves,[27] increasing the transporter thermodynamic stability (also observed for vitamin B12 importer homodimer, BtuCD).[28] Other studies suggested that this DBP would be water-filled, serving as a pathway to the substrate efflux.[29] In fact, the existence of a dual pseudosymmetric translocation pathway for the above-mentioned H and R sites was later described in 2011.[16]

However, it was the publication in 2009 of the murine crystallographic structure (PDB ID: 3G5U),[30,31] with a higher resolution (3.8 Å), that clarified Pgp's structural properties. A large internal chamber of approximately 6000 Å^3 was defined as the drug-binding pocket, opening to the intracellular compartment and the lipid membrane through two 'gates' formed by the pairs TMD 4/6 and 10/12. Seventy-three inward-facing residues were identified, and three distinct drug-binding sites, located in the outer leaflet of the lipid bilayer, were proposed based on the residues chemical characteristics and docked structures of the cyclic peptide stereoisomer's QZ59-RRR and QZ59-SSS.[31] These sites occur at the opposite side regarding H and R sites, located next to the inner leaflet/water interface. For QZ59-RRR, the interaction site is found next to TMDs 1, 5, 6, 7, 11, and 12 and is mainly mediated by hydrophobic residues (Table 1).[31] In the case of QZ59-SSS, two binding sites were found between TMDs 1, 3, 6, 7, 11, and 12 ('upper' site) or TMDs 1, 5, 6, 7, 8, 9, 11, and 12 ('lower' site), including three additional residues: Gln721, Gln986, and Ser989. The same study also identified Phe728 and Val982 (in human Pgp) as central for drug binding, characterizing the 'upper' section of the DBP as more hydrophobic in contrast with a more polar section of DBP, near the inner leaflet interface.

Table 1. Residues Identified To Interact with Modulators QZ59-RRR and QZ59-SSS (Adapted from Aller et al., 2009)

QZ59-RRR		QZ59-SSS	
Met68	Phe724	Met68	Tyr949
Tyr303	Phe728	Leu300	Phe974
Phe332	Tyr949	Tyr303	Val978
Leu335	Phe974	Phe332	Ala981
Ile336	Ser975	Ile336	Met982
Phe339	Val978	Phe339	Gly985
Gln721		Gln721[a]	Gln986[a]
		Phe724	Ser989[a]
		Phe728	

[a]Mapped in the 'lower' site only.

Docking studies were also performed aiming to identify residues essential for the interaction with Pgp efflux modulators. Jabeen et al.,[32] from a set of enantiopure benzopyrano[3,4-b][1,4]oxazines, identified the flexibility of these molecules as a determinant factor for the activity of the diastereoisomers. When compared with QZ59 isomers, an enhanced stereoselectivity, similar interactions, and increased contacts with residues in TMDs 4, 5, and 6 were found, which is in accordance with previous studies.[31,33−35] These results agreed with the existence of a dual pseudosymmetric translocation pathway, previously suggested by Loo et al.[29] and experimentally supported by Parveen et al.[16] A different study by Dolghih et al.[36] tested the 'induced-fit' model proposed by Loo et al.[22] with a series of well-known substrates and inhibitors of Pgp. Data from efflux studies, calcein inhibition assays, and blind tests with protease inhibitors were used to develop a method suitable to predict substrate binding to Pgp. They found that the flexibility of the cavity is also critical, although they also assumed that the results could be explained by the low resolution of the crystal structure. For modulators, relevant changes in the side chain positions were found for residues Phe71, Phe332, and Phe728.

So far, the only direct structural information about the interaction between modulators and Pgp was obtained by Aller et al., allowing a characterization of three drug-binding sites and corresponding residues. Since no structure with cocrystallized substrates is available, no direct determination of the position of substrate-binding sites (SBSs) was possible. On the other hand, the quality of the results obtained by molecular docking may suffer from the low crystallographic resolution of the structure, from the absence of a lipid bilayer (that may change TMDs packing) and from the absence of a 'linker', proved important for substrate specificity and activity[37,38] but also because this structure defines the lower pocket boundary (allowing a correct

cavity search) and stabilizes Pgp's nucleotide-binding domains.[39] In 2012, our group published a series of molecular dynamics (MD) simulations,[40] based on the available murine crystallographic data, which addressed these issues.

In the MD simulations, the missing 'linker' was built, added, and equilibrated with the crystallographic structure, allowing for the first time a clearer definition of the DBP lower boundary (next to the inner leaflet interface). The whole structure was then fully solvated and equilibrated in the presence of an adequate lipid bilayer.[40] This new structure showed remarkable asymmetries in the behavior of the 'entrance' gates formed by TMDs 4/6 and 10/12 with only one entrance gate to the DBP, in accordance with the latest published Pgp crystallographic structure (from *Caenorhabditis elegans*, by Jin et al.[41]). In addition, several MD simulations were made with molecules placed in different positions inside the DBP (inhibitors and substrates). Even in this water-filled DBP, ligand-protein interactions occurred extensively with residues TMDs 1−3, 5−7, and 10−12, in agreement with previously described experimental studies.[29,31,32] As such, the definition of the DBP lower boundary is of great importance for the identification and characterization of the H and R sites.

In this paper we describe a series of docking studies comprising a database of 68 molecules (substrates, modulators, efflux probes and lipids). The main objective is to clearly define, for the first time, the location and lining residues for the three different sites inside Pgp's drug-binding pocket and to propose a classification scheme able to distinguish modulators from substrates.

MATERIAL AND METHODS

Databases. *Substrates* (N = 32) were selected according to the classification by Polli et al.[42] and later reviewed by Rautio et al.,[43] based on results obtained in cell monolayer efflux, ATPase, and calcein-AM fluorescence assays. Rhodamine-123, digoxin, and calcein-AM, frequently used as efflux probes,[43] were grouped in *probes* (N = 10) along with some of the most important digoxin and calcein-AM metabolites and rhodamine derivatives with modulatory capability. *Modulators* (N = 19) were compiled from available literature and grouped in a distinct category. To evaluate Pgp's flippase capability, a *lipids* database (N = 7) comprising common phospholipid molecules, also including cholesterol was also built (not used in pocket assignments).

Docking Studies. Molecular docking was made with a refined murine P-glycoprotein[40] derived from the original crystallographic data, comprising 100% identity between mouse and human structures for the residues inside the DBP. MarvinSketch v5.11.1[44] was used for drawing structures. All ligands were then exported to MOE v2010.10,[45] minimized with the MMFF94x force-field (adjusting hydrogen and lone pairs by default), and exported as mol2 files. PDBQT files were generated with AutoDockTools v1.5.6rc2[46,47] for further utilization in AutoDock VINA 1.1.2[48] docking software. The binding location was defined by a docking box including the whole internal cavity defined by Aller et al.,[31] centered at the DBP and with dimensions *xyz* of 35.25, 25.50, and 45.25 Å, respectively (*xy* corresponds to the membrane plane). Due to the large search space volume (over 40.000 Å^3), 'exhaustiveness' parameter was manually set to 50. Visual inspection of the docking poses was made in MOE to allow the identification of individual docking zones.

Identification of Drug-Binding Pockets. Although it was experimentally demonstrated that the H and R sites are located next to the inner leaflet interface of the membrane bilayer, little information exists relating residues to sites. Using the Pgp refined structure, a cavity search was performed with EPOS^{BP} software,[49,50] (default parameters) over the whole drug-binding pocket.

The top-ranked pose of each molecule in each zone was then overlapped with the cavity search results (by EPOS^{BP}), identifying lining atoms (within a distance of 5 Å from the pocket probes), and calculating mean pocket volume and polarity (ratio of the sum of N, O, and S atoms to the sum of N, O, S, and C atoms).[51] Graphical images of the docking poses, pocket residues, and molecular/electrostatic maps of the pocket surfaces were made in MOE.

Pocket Assignment. The identified drug-binding pockets were defined as substrate- or modulator-binding sites according to the molecules that preferentially docked in each location. Similarly to Shapiro et al.,[14,15] the substrate-binding sites H and R started to be assigned from top ranked docking poses of Hoechst 33342 and rhodamine-123 respectively. Other experimentally assigned molecules were also used in DBS identification. In a similar way as in the studies by Loo and Clarke,[18,22,24] the modulator-binding (M) site was identified based on the interaction with verapamil (top-ranked docking poses).

Generation of a Classification Scheme. For each DBS, ligand-protein contacts were evaluated through the analysis of all top-ranked docking poses. The number of residues, nature, and maximum number of established interactions (nonbonded and hydrogen bonds) were assessed through the LIGPLOT[52] and HBPLUS[53] software. A classification scheme was then developed based on binding energies (ΔG) and cross interaction capability in order to classify each molecule as substrate or modulator.

RESULTS

Identification of Drug-Binding Sites. A large number of published studies identified three major drug-binding sites in Pgp, based on experiments with verapamil (gold-standard modulator), Hoechst 33342, and rhodamine-123 (substrates). Two of them were named the H-site and the R-site by Shapiro and Ling[14,15] after identifying Hoechst 33342 and rhodamine-123 as preferential substrates for each, respectively. Additionally, they also suggested that both sites could interact in a positively cooperative manner, thus affecting the substrate efflux.[14]

In our study, the whole internal drug-binding pocket was defined as the docking box. The nine best ranked docking poses obtained for verapamil, rhodamine-123, and Hoechst 33342 distinctly outlined two out of three major drug-binding sites (Figure 1). Regarding verapamil, this molecule docked in two major locations. Four poses, with binding energies from −7.6 to −7.4 kcal·mol^{-1}, docked at the top of the cavity located next to the outer leaflet of the lipid bilayer, in a site first described by Aller et al.[31] based on a murine Pgp structure with two cocrystallized modulators (QZ59-SSS and QZ59-RRR)—hereafter named the M-site. Additionally, five docking poses were registered at a lower location, next to the inner leaflet interface, with binding energies ranging from −7.6 to −7.3 kcal·mol^{-1}.

Verapamil is often described in the literature as substrate[54−56] or modulator[2,54,57] but, assuming that the lower

dx.doi.org/10.1021/ci400195v | J. Chem. Inf. Model. 2013, 53, 1747−1760

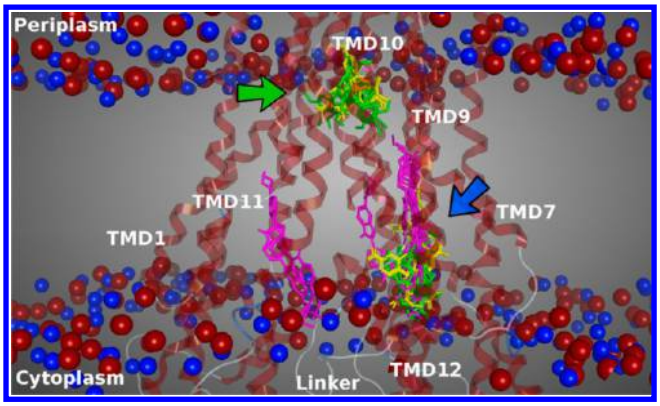

Figure 1. Best ranked docking poses for verapamil (green), rhodamine-123 (yellow), and Hoechst 33342 (pink), allowing the M-site (green arrow) and the R-site (blue arrow) assignments. Phosphate (red) and nitrogen (blue) atoms of lipid headgroups are also represented as a way to assess the relative position of the lipid membrane.

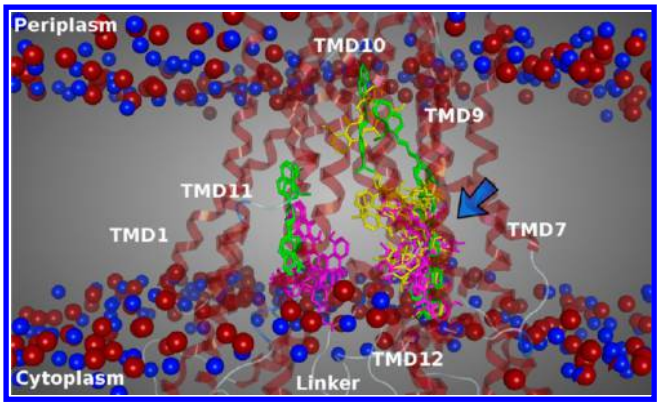

Figure 2. Best ranked docking poses for LDS-751 (green), daunorubicin (yellow), and doxorubicin (pink). The R-site is identified by a blue arrow. Phosphate (red) and nitrogen (blue) atoms of lipid headgroups are also represented as a way to assess the relative position of the lipid membrane.

location detected next to cytoplasmic interface is a substrate binding site, the identical binding energies at both sites can provide an initial clue for the promiscuous behavior of verapamil. In addition, the docking poses of rhodamine-123 were also found at the top and bottom locations, with equal binding energies of −9.2 kcal·mol^{-1}. This finding supports the cytoplasmic inner leaflet C-terminal position as a substrate-binding site, described in the literature as the location where rhodamine-123 interacts— R-site. Therefore, verapamil and rhodamine-123 poses allowed a first insight about the boundaries of the R-site (Figure 1).

For Hoechst 33349, however, almost all of the top-ranked docking poses were found at the assigned R-site (−10.5 kcal·mol^{-1}), with only two poses registered at the N-terminal halve in a symmetrical location, although with lower binding energy (−9.0 kcal/mol − Figure 1). This result did not allow a positive identification of the H-site location. Nonetheless, several studies corroborate the N-terminal location as a possible H-site. Pajeva et al. identified two possible locations for the H-site next to TMD5 and TMD11,[35] based on a pharmacophore model of Hoechst 33342. Loo and Clarke, through cysteine scanning mutagenesis,[58−60] showed that TMDs 6, 9, and 12 formed the R-site and TMDs 2, 3, 4, 10, and 11 delimited the H-site. Both studies are consistent with our R-site assignment, and, therefore, the symmetrical position located next to TMDs 2, 3, 4, 10, and 11 can be assigned as the H-site. In addition, Qu and Sharom mapped the H-site 10−14 Å below the membrane surface,[61] locating LDS-751 binding site closer to the cytoplasmatic membrane/water interface regarding the Hoechst 33342 binding site.[21] In our study, and for the two identified substrate-binding sites, the assigned H-site is indeed more deeply buried in the cytoplasmatic leaflet of the membrane (2.4 Å for the water/lipid interface against 0.5 Å mapped for the R-site).

Another way to validate the assignment of H and R sites is to analyze docking poses for additional molecules as anthracyclines[14] and LDS-751 (described to preferably bind to the R-site[15]), quercetin and colchicine (bind to the H-site[14]), and vinblastine, actinomycin D, and etoposide (bind in both sites[14]). Our docking study showed, for LDS-751 (Figure 2), docking poses at the assigned R-site (top-ranked pose, −8.1 kcal·mol^{-1}) and the H-site (−7.9 kcal·mol^{-1}) but also at the M-site (−7.8 kcal·mol^{-1}). For anthracyclines (daunorubicin and doxorubicin), the top-ranked docking poses were found at the assigned R-site (Figure 2) with binding energies of −10.2 and −10.1 kcal·mol^{-1}, respectively. Although daunorubicin almost exclusively docked at the R-site (only 1 pose registered at the M-site with −8.8 kcal·mol^{-1}), doxorubicin displayed three poses at the H-site, with affinities ranging from −9.4 to −9.2 kcal·mol^{-1}.

Since Hoechst 33342 and doxorubicin docked in both H and R sites within the standard error reported for VINA (2.85 kcal·mol^{-1}),[48] this does not allow for discriminatation between sites. However, these global results are in accordance with previous experimental findings[14] which claimed that molecules interacting at the H-site will positively affect the efflux from the R-site and vice versa. Specifically for Hoechst 33342, and as demonstrated by Shapiro and Ling,[14] low doxorubicin concentrations may effectively stimulate the efflux from the H-site translocation pathway, whereas at higher concentrations the competition between both molecules increases, having as consequence efflux impairment. Finally, etoposide was also found at both sites (with ΔG of −10.0 and −9.5 kcal·mol^{-1} for R and H sites, respectively), and vinblastine (−8.6 kcal·mol^{-1}) and actinomycin D (−11.2 kcal·mol$^{-1)}$ top-ranked poses were found at the assigned H-site (Figure 3). Hence, the symmetrical positions in which these molecules docked (near the inner leaflet interface) strongly corroborate our H and R sites assignment hereby proposed.

Quercetin and colchicine, on the other hand, did not dock preferentially at the assigned H-site, instead being found at the M-site and the R-site with similar binding energies (difference of 0.3 kcal·mol^{-1} between sites). Although different from the results reported by Shapiro and Ling,[14] the docking results are in accordance with several experimental results in which colchicine was shown to protect residues in TMD6 and TMD12 (belonging to the R-site) from dibromobimane labeling.[62,63] Quercetin and colchicine also compete with [^{3}H]azidopine for Pgp labeling, a substrate proved to interact in a similar location as calcium channel blockers like verapamil[64,65] and different from cyclosporine A or vinblastine.[66] In addition, quercetin has a large number of cellular targets and is also severely affected by the type of phospholipid and protein/phospholipid ratio.[64] Therefore, it is not clear that quercetin and colchicine bind preferentially at the H-site or if

dx.doi.org/10.1021/ci400195v | J. Chem. Inf. Model. 2013, 53, 1747−1760

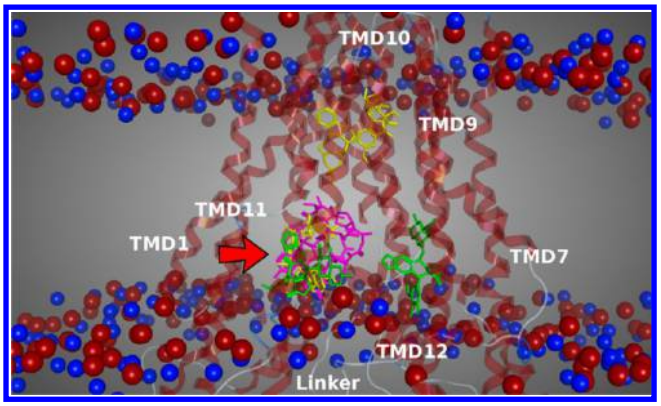

Figure 3. Docking poses for etoposide (green), vinblastine (yellow), and actinomycin D (pink). The H-site is identified by a red arrow. Phosphate (red) and nitrogen (blue) atoms of lipid headgroups are also represented as a way to assess the relative position of the lipid membrane.

their influence in rhodamine-123 efflux can be exerted by other mechanisms.

Based on the above data, a question remains: how can these results explain the rhodamine-123 efflux increase in the presence of colchicine and quercetin and simultaneously affect Hoechst efflux? A direct competition between rhodamine-123, quercetin, and colchicine may favor rhodamine-123 efflux by displacing colchicines and quercetin into the alternative H-site pathway (impairing Hoechst 33342 efflux). However, another suitable response can be found in the minipharmacokinetic system proposed by Didziapetris et al.[67] in which essential prerequisites for any Pgp substrate are molecular weight (MW) > 400 and a Lipinsky number of acceptors (LA) ≥ 8. It is clear that none of the considered molecules (rhodamine-123, quercetin, or colchicine) fully comply with these specifications. Nonetheless, the combined properties of such small molecules may have a positive influence in the stimulation of drug efflux at one of the translocation pathways.

All of the above data thoroughly supports the logical assignment of these three major drug-binding sites within Pgp's drug-binding pocket, corroborating the earlier identification by Aller et al. of a modulator-binding site (M-site) and, for the first time to our knowledge, assigning the substrate-binding H-site and R-site to specific locations within the internal cavity.

DBS Characterization. After the identification of three major drug-binding locations at the Pgp's internal pocket, a thoughtful characterization of the lining residues, volume, and polarity followed. One of the first noticeable differences between the M-site and H/R drug-binding sites is the amino acid composition (Table 2).

At the M-site, 33% of residues have aromatic side chains (namely phenylalanine and tyrosine) against 15 ± 1% in the substrate DBSs. Although the number of hydrophobic residues is similar in all sites (40 ± 1%), polar residues are predominantly found at the H- and R-sites (44 ± 1% against 27% in the M-site). This asymmetry in residues distribution, already described by Aller et al.,[31] has a direct effect in the DBS mean polarities with calculated values of +0.24 for the M-site, +0.32 for the R-site, and +0.33 for the H-site. The analysis also revealed that three residues in the linker's upper loop are common to H- and R-sites, thus supporting the importance of this structure for the structural recognition of substrates.[37] Since several other residues are also common to both substrate-

Table 2. Mapped Residues for Each DBS[a]

M-site (n = 33)		R-site (n = 49)		H-site (n = 45)	
His60	*Phe339*	Ala229	Leu720	*His60*	*Gln343*
Leu64	*Gln721*	Thr236	*Gln721*	*Val121*	*Ser345*
Met67	*Phe724*	Asp237	*Phe724*	Leu122	*Pro346*
Met68	Ser725	Leu240	Ser762	Ala125	Asn347
Phe71	Phe728	His241	Thr765	Gln128	*Glu349*
Gly72	Ser729	Ile289	Phe766	Val129	Ala350
Thr75	Val732	Asn292	Gln769	Trp132	Ala351
Tyr113	*Gln942*	Met295	Glu770	Cys133	*Arg676*
Val121	Met945	Gly296	Phe773	Asn179	Lys677
Tyr303	*Tyr946*	Phe299	Gly774	Glu180	Leu678
Gln326	Tyr949	Leu300	Glu778	Gly181	Leu875
Val327	Leu971	*Ile336*	Ala819	Ile182	Ser876
Leu328	Phe974	*Phe339*	Gln820	Gly183	Leu880
Thr329	Ser975	*Ser340*	Val821	Asp184	Ala897
Phe332	Val978	*Val341*	Lys822	Ile186	Lys930
Ser333	Met982	Gly342	Gly823	Gly187	Phe934
Ile336		*Gln343*	Gly985	Met188	Phe938
		Ala344	Gln986	Phe190	Ser939
		Ser345	Ser988	Gln191	*Gln942*
		Pro346	Ser989	His241	Ala943
		Glu349	Phe990	*Ser340*	*Tyr946*
		Gln674	Ala991	*Val341*	*Asp993*
		Asn675	Pro992		Lys996
		Arg676	*Asp993*		
		Asn717			

[a]Residues in *italic* are common to at least two DBS, and underlined residues are part of the linker sequence.

binding sites (Table 2), this structural finding can be a link to the positively cooperative assumption by Shapiro and Ling.

This difference in the polarity and electrostatic potential between the modulator site and substrate-binding sites could also be inferred from the residues distribution pattern at the M-site (Chart 1). The M-site registers an increased percentage of

Chart 1. Residues Distribution Percentage for Each Site

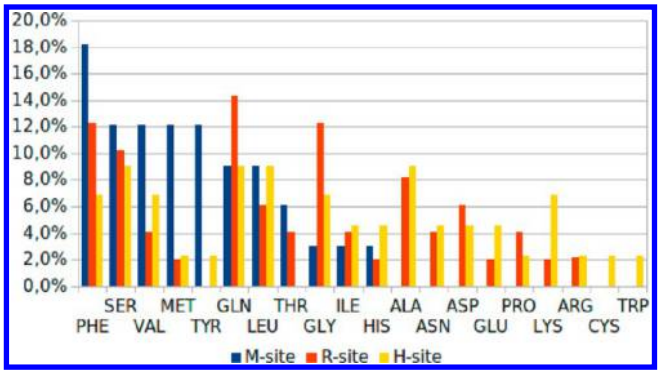

aromatic and hydrophobic residues (phenylalanine, valine, methionine, and tyrosine), whereas the residues distribution between H- and R-sites are similar, with an increased prevalence of more polar aminoacids such as glutamines or glycines at the R-site and cysteine or tryptophane only found at the H-site. Serines and leucines, however, show similar distributions throughout the pockets.

dx.doi.org/10.1021/ci400195v | J. Chem. Inf. Model. 2013, 53, 1747−1760

The affinity differences toward drug molecules between H- and R-sites may be explained by some asymmetry in the residues distribution. For instance, the H-site has a higher percentage of charged residues (lysine, histidine, and glutamic acid residues), whereas the R-site has a higher number of glycines, glutamines, and prolines (nonionizable residues). Interestingly, no threonines and tyrosines are found in H- and R-sites, respectively.

For all three DBS, pocket volumes were also calculated by probing the internal space with EPOS^{BP} software. A mean volume of 1300 ± 300 Å^3 was estimated for the M-site, whereas the calculated mean volume for both substrate-binding sites were considerably higher, 1900 ± 500 and 2200 ± 600 Å^3 for R- and H-sites, respectively (30% and 39% higher, respectively).

A graphical representation of the Molecular Surface (MS) for the M-site (Figure 4, top left) shows a 'bell-shaped' structure at the top of the DBP, opening directly into the internal cavity. The correspondent Electrostatic Map (EM − Figure 4, top right) revealed a mainly hydrophobic surface, with π electrons from aromatic rings arising as contact surfaces with an electron-donating potential and four extra electron-acceptor surfaces found near hydroxyl and amino groups of residues Gln326, Gln721, Ser725, and Tyr946.

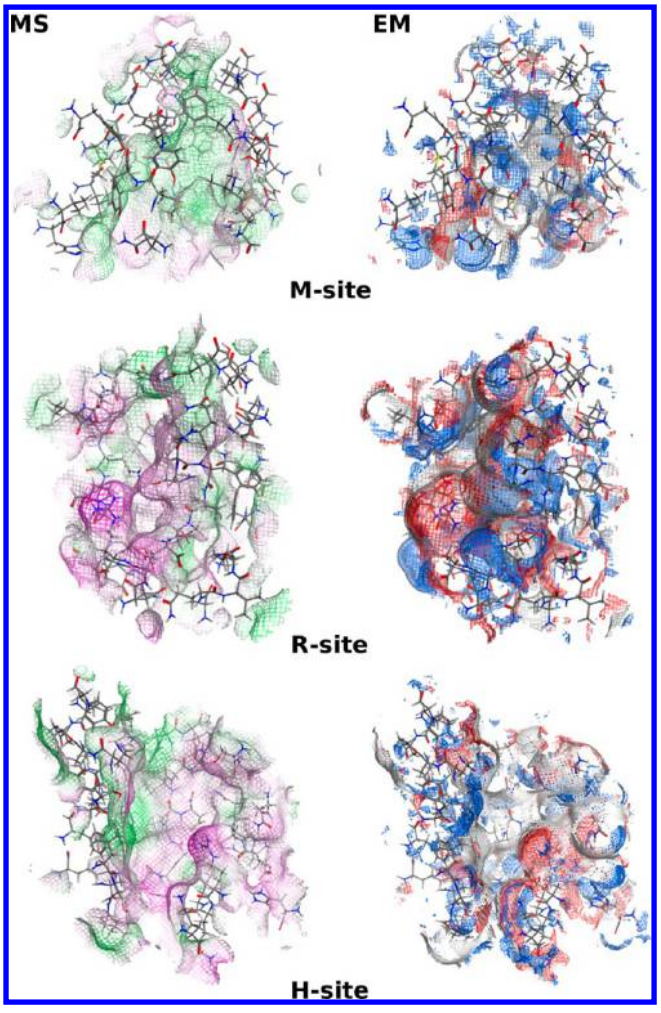

Figure 4. Graphical representation of the Molecular Surface (MS—green, hydrophobic and pink, polar) and Electrostatic Map (EM—blue, electron donor; gray, neutral and red, electron acceptor) for the identified drug-binding sites.

The R-site showed a more 'pouch-shaped' like cavity (Figure 4, middle left), with the pocket entrance surrounded by polar residues (Ser340, Arg676, Gln721, Ser988, and Ser989) and two aromatic residues (Phe339 and Phe756) contributing to a hydrophobic region next to the pocket entrance. The EM shows an increased proportion of charged surfaces (Figure 4, middle right), with electron-donating carbonyl and hydroxyl groups of residues Gln769, Ser988, Ser989, and Phe990 spanning through a wide surface, further extended by the aromatic side chain of residue Phe773. On the contrary, Arg676 and Gln721 have electron-accepting characteristics and are located next to the cavity entrance.

Interestingly, for the H-site, the most noticeable feature is the direct access from the 'entrance-gate' between TMD10/12. Hence, in this study the H-site is much more accessible to any molecule that leaves the inner leaflet into the DBP (Figure 4, bottom left). The cavity surface is much more hydrophobic when compared with the R-site, having a hydrophobic cleft ranging residues Val129, Trp132, Phe934, and Phe938. Toward the R-site, a more polar cleft extends through TMD3, from residue Asn179 to Gly181, ending at Ser340 (common with the R-site). The EM (Figure 4, bottom right) shows a more positively charged domain formed by residue Arg676 (linker) and Lys996 (TMD12) against two negative contact points, formed by Glu180 (TMD3), Ser939 and Gln942 (TMD11).

The statement that only the H-site is directly accessible from the lipid bilayer must be considered with caution. Many studies clarified that Pgp efflux tends to occur in an alternate way, with NBD1 and NBD2 hydrolyzing ATP in a sequential mode at different points of the efflux cycle.[68−71] Our previous study[40] showed that NBD2 can more easily accept an ATP molecule. However, it is possible that this particular configuration would change when NBD1 is the one involved in nucleotide hydrolysis, shifting the 'entrance gate' to the gap between TMD 4/6 and creating a direct access into the R-site.

Classification Scheme Development. Having positively identified and characterized the three major drug-binding sites within the Pgp internal cavity, we carried out further docking studies with molecules classified as substrates or modulators by Polli et al. and later re-evaluated by Rautio et al. (*substrates*, N = 32). Three additional groups, comprising known Pgp modulators (*modulators*, N = 19), molecules used as efflux probes (*probes*, N = 10), and phospholipid molecules (*lipids*, N = 7), were added to the initial data set.

At this point, it is imperative to define the concept of Pgp efflux modulation. Experimentally, the modulation ability is evaluated through several experimental methods such as cell monolayer efflux studies (digoxin, calcein-AM, prazosin, vinblastine, or colchicine),[43] calcein-AM efflux inhibition,[42] drug-stimulated Pgp ATPase quantification,[42] and rhodamine-123 accumulation assays.[72] Therefore, the affinity of probe substrates for drug-binding sites in Pgp affects the outcome, for any evaluated molecule. An example is the experimentally determined effect of daunorubicin and colchicine on rhodamine-123 efflux. In our study, daunorubicin has a low binding free energy (−10.2 kcal·mol^{-1}). This may favor a direct competition with rhodamine-123 (−9.2 kcal·mol^{-1}) for the R-site, having as consequence a decrease in the rhodamine's efflux rate, dependent on the daunorubicin concentration. For colchicine, with a higher ΔG (−8.4 kcal·mol^{-1}), the R-site competition favors rhodamine-123, displaces colchicine to the

Scheme 1. Classification Scheme for Pgp Substrates

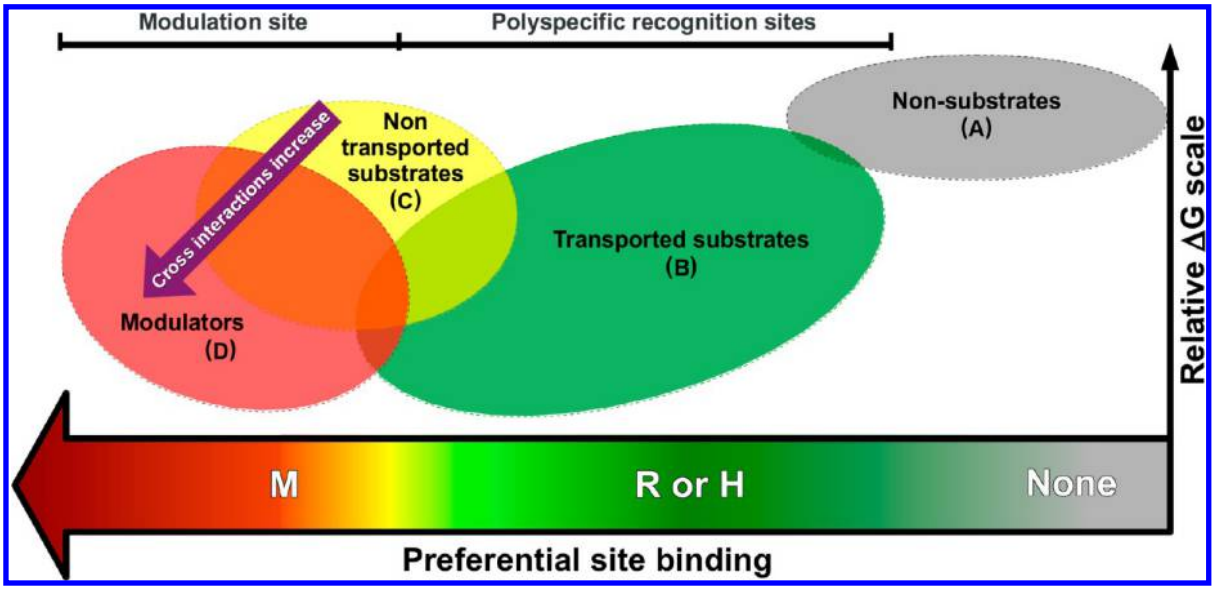

alternative translocation pathway and decreasing Hoechst 33342 efflux (as observed experimentally by Shapiro and Ling).[14] This model can also explain the modulation observed by actinomycin D (−11.2 kcal·mol^{-1}), in which a direct competition for the H-site will reduce Hoechst 33342 efflux, displacing it to the R-site translocation pathway and increasing the competition of Hoechst 33342 with rhodamine-123. For etoposide, with lower binding free energies for both sites than rhodamine-123 (−10.0 and −9.5 kcal·mol^{-1} for R- and H-sites, respectively), both translocation pathways can be directly affected.

Other possible way to modulate Pgp efflux is through allosteric influence of a given molecule at the M-site, recently characterized as a central modulator drug-binding site.[31,73] Surprisingly, many molecules found in the literature are simultaneously described as substrates and modulators. Even proven substrates such as vinblastine seem to have modulatory activities, being classified as Pgp substrate but also being frequently referred to in the literature as efflux modulator for colchicine/digoxin[43] and rhodamine-123.[74] Moreover, vinblastine is also capable of self-modulation (IC_{50} of 89.7 μM).[43]

Shapiro and Ling demonstrated experimentally that vinblastine can inhibit the efflux of rhodamine-123 and Hoechst 33342,[14] providing an explanation based on equal affinities for both H- and R-sites. However, according to our results, a different proposal can be suggested. Vinblastine's top-ranked poses were found at the H-site and also at the M-site. Unlike etoposide and actinomycin D, the vinblastine's poses at the M-site were found to allow the formation of hydrogen and nonbonded interactions between both halves of Pgp i.e. cross interactions. The number, type, and distribution of these cross interactions between both halves can have an impact on conformational changes following ATP binding, impairing Pgp opening and modulating Pgp efflux.

As already stated, verapamil is another example of a molecule ambiguously identified as modulator and substrate. In our previous work,[40] we characterized verapamil as a modulator, in an intermediate level between substrates and inhibitors. In the present study, verapamil top-ranked poses at M- and R-sites have the same energy (−7.6 kcal·mol^{-1}), not allowing a direct identification as modulator or substrate. However, the analysis of the interaction pattern between both halves at the M-site identified a high capability for cross interaction formation, thus supporting verapamil as a modulator rather than a substrate, corroborating our previous findings.

The above-described insights allowed a simpler interpretation of some aspects of Pgp's efflux process. For instance, in the experimental methodologies the cellular line is selected with caution, whereas probe molecules are frequently selected based solely on their efflux ability by Pgp. In addition, it seems that some molecules frequently characterized as substrates (e.g., vinblastine, paclitaxel, and ritonavir) also have some modulatory ability. The present docking results identified the formation of hydrogen-bond and nonbonded interactions between both halves of Pgp, exclusively at the M-site, as a possible explanation for the modulation effect of some molecules. These findings lead to the introduction of an alternative classification, solely based on docking binding energies and cross interaction capability at the M-site. This classification is not dependent on the use of probes, thus allowing a better clarification of the preferred interaction sites and the molecules ability to compete for substrate-binding sites or to establish cross interactions between both halves (Scheme 1).

This classification scheme contains four main categories:

(A) *Nonsubstrates*, molecules with an estimated binding energy higher than −7.0 kcal·mol^{-1} (not likely to interact with Pgp).

(B) *Transported substrates*, molecules with increased preference (lower ΔG) for substrate-binding H- and R-sites and, if any docking pose at the M-site, with weak cross interaction capability;

(C) *Nontransported substrates*, molecules with a slightly higher preference for the M-site rather than H- and R-sites, yet with weak cross interaction ability;

(D) *Modulators*, molecules with lower ΔG and increased preference for the M-site, also able to establish a strong cross interaction effect;

The definition of Pgp modulator or Pgp inhibitor remains unclear throughout the literature. As fully competitive inhibition of Pgp transport is yet to be achieved, the developed classification scheme aims to clarify the molecules affinity

dx.doi.org/10.1021/ci400195v | J. Chem. Inf. Model. 2013, 53, 1747−1760

toward the substrate-binding sites (ability to be effluxed i.e. transported substrates), against other molecules that have a weak (nontransported substrates) or strong (modulators) impact on Pgp efflux due to their cross interaction capability.

Classification of Pgp Substrates. Using this classification, a thorough analysis of the databases was performed. For *modulators* (N = 19, Supporting Information − Table S1), 14 molecules (74%, ΔG from −7.9 to −11.2 kcal·mol^{-1}) had the top-ranked pose at the M-site and only 5 (26%, −7.9 to −11.1 kcal·mol^{-1}) at the R-site or the H-site. This seems to reveal an increased preference of most modulators toward the more hydrophobic drug-binding site (M-site). For *substrates* (N = 32, Supporting Information − Table S2), the top-ranked docking poses for 20 molecules (63%) were in substrate-binding sites, 8 (25%) were observed at the M-site and 4 (12%) had identical binding energies for M-, H-, or R-sites. Regarding the *probes* group (N = 10), 5 molecules (50%) had their top-ranked docking pose in the R-site, 2 (20%) in the M-site, and 3 (30%) showed the same binding affinity for SBSs and the M-site (Supporting Information − Table S3). Interestingly, for *lipids* (N = 7, Supporting Information − Table S4), the binding energies registered were all above −7.0 kcal·mol^{-1} (except cholesterol). Therefore, and according to the classification scheme, they cannot be considered substrates for Pgp, not corroborating the lipid flippase model as a possible mechanism of action for Pgp.

Nonsubstrates (A). In an attempt to define possible nonsubstrates, an empirical cutoff value had to be established (−7.0 kcal·mol^{-1}), thus separating this class from all others. Within this group, only diphenhydramine, trimethoprim, and chloroquine were classified as nonsubstrates. According to several studies, only the first two are classified as nonsubstrates.[75,76] Chloroquine, however, is described to partially reverse MDR but not to inhibit Pgp photolabeling.[77] Due to the high binding energy found in this study, it is conceivable that chloroquine may act in a different target[78] than Pgp.

Transported Substrates (B). Nine molecules, including doxorubicin, etoposide, and Hoechst 33342, were found to dock exclusively in both SBSs with binding affinities between −10.5 and −9.0 kcal·mol^{-1}. Daunorubicin, progesterone, and LDS-751 additionally registered at least one pose at the M-site, however, with a weak cross interaction capability. Methotrexate (MTX), frequently referred to as a nonsubstrate, docked exclusively at the R-site (−8.6 kcal·mol^{-1}). It is known that this molecule has an active carrier-mediated influx that allows the accumulation of MTX within the cell. However, in carrier-deficient cells it was additionally found that MTX is actively effluxed by Pgp,[79−81] thus supporting our findings.

Cyclosporine A was found exclusively at the H-site, yet this molecule is referred to as a potent inhibitor with IC_{50} values ranging from 1.4 to 6.2 μM.[43] In this study, cyclosporine A registered a high binding energy (−7.9 kcal·mol^{-1}) toward the H-site, higher than most substrates. In addition, cyclosporine A is the molecule with the highest molecular volume (1721 Å^3, calculated with MOE). When taking into account the volume for M-, R-, and H-sites estimated earlier, the only site in which cyclosporine A may fit is the H-site. Indeed, this fact is shown by our model (Figure 5) in which cyclosporine fully occupies the whole H-site and part of the entrance gate. For this particular case of large molecules, and based on our docking findings, Pgp inhibition may be achieved through a nonspecific bulk mechanism by which the access to the internal drug-binding pocket of Pgp becomes blocked. Actinomycin D, in a similar way as cyclosporine, is also a large molecule (1645 Å^3) that is only found at the H-site (−11.2 kcal·mol^{-1}) and may also act through this mechanism.

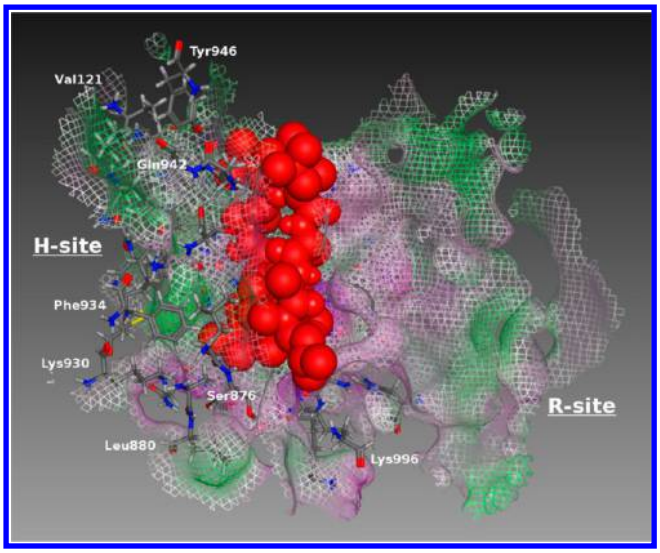

Figure 5. Cyclosporine A (space fill, red) at the H-site.

Nontransported Substrates (C). Six molecules were identified, all showing lower binding energies for the M-site between −9.1 kcal·mol^{-1} (itraconazole) and −7.9 kcal·mol^{-1} (QZ59-RRR) when compared with *transported substrates (B)*. Within this group, differences were found addressing the Pgp's stereospecificity. QZ59-RRR (IC_{50} = 4.8 μM) showed a weaker cross interaction effect when compared with QZ59-SSS (IC_{50} = 1.2 μM).[31] For mefloquine enantiomers (IC_{50} = 1−10 μM),[82] (-)-mefloquine also had a weak cross interaction effect when compared to (+)-mefloquine, in accordance with at least one experimental study that showed higher activity for the latter.[83] Interestingly, no stereospecific effect was observed for flupentixol enantiomers, thus corroborating their similar activity (IC_{50} = 24 and 25 μM for isomers Z and E, respectively).[84]

Although colchicine is considered a Pgp substrate, several experimental studies showed some degree of modulatory activity in many cell lines (IC_{50} from 89 μM[85,86] to 230 μM[87]). According to our model, this can be explained due to a weak cross interaction capability displayed by the poses found at the M-site. Itraconazole, with identical binding energies for the H-site and the M-site and a moderate cross interaction capability, shows an increased efflux modulation capability (IC_{50} = 1.6 μM).[88,89] It is interesting to note that for this class (*nontransported substrates*), with the exception of the QZ59 molecule, the activity increases with log P.

Modulators (D). This group comprises 8 molecules with binding affinities ranging from −7.9 to −11.5 kcal·mol^{-1} at the M-site. Laniquidar (EC_{50} of 510 nM),[90,91] latilagascene D (IC_{50} unknown),[92] and zosuquidar (IC_{50}= 60 nM),[93] are some of the most potent Pgp modulators included in this group. Midazolam (IC_{50}= 10 μM,[85,86] −9.1 kcal·mol^{-1}), QB13 (IC_{50}= 1.0 μM,[94] −8.9 kcal·mol^{-1}), and (S)-methadone (IC_{50}= 7.5 μM,[95] −7.9 kcal·mol^{-1}) are the ones within this category with the lowest activity. Surprisingly, paclitaxel and amprenavir are also part of this group, due to their strong M-site cross interaction capability.

Paclitaxel is included in this group due to the lowest binding energy registered in this study (−11.5 kcal·mol^{-1}). Although frequently referred to as a substrate, several studies identified

dx.doi.org/10.1021/ci400195v | J. Chem. Inf. Model. 2013, 53, 1747−1760

this molecule as a potential modulator on several cell lines (IC_{50} from 1.2 to 54 μM).[74,85,87] In addition, the inhibition potential of the taxane scaffold was demonstrated through the utilization of a library of noncytotoxic taxane-based reversal agents (tRAs), in which doxorubicin and mitoxantrone efflux were strongly modulated in Pgp, MRP1, and BCRP.[96]

Amprenavir (IC_{50} of 8.6 μM)[97] is also able to establish strong cross interactions between both halves of Pgp but with a higher binding energy at the M-site (−8.9 kcal·mol^{-1}) and similar binding energies for the R-site top-ranked pose (−8.5 kcal·mol^{-1}). Interestingly, the multidrug-reversal activity of several antiretrovirals was recently evaluated by docking against the crystallographic murine Pgp structure. The conclusion was that ritonavir (IC_{50} of 1.29 μM)[97] is a more potent Pgp inhibitor than amprenavir,[98] with a lower Glide SP docking score when compared with amprenavir. A similar result was obtained with VINA in the study herein, having ritonavir obtained lower M-site binding energies in comparison with amprenavir.

Intersections. Twenty-four molecules (35%), however, cannot be unambiguously included in any of the above groups due to small differences in binding energies between all three sites. Although no conclusive identification as substrate or modulator could be achieved, the calculated cross interaction capabilities for the M-site poses are a suitable indicator for the modulation capability of these molecules. Our study shows that cross interaction capability tends to increase from *transported substrates* (B) to *nontransported substrates* (C), associated with a progressive shift of the top-ranked binding pose from the SBSs to the M-site (lower ΔG values). Similarly, from *nontransported substrates* (C) to *modulators* (D), the cross interaction capability increases inversely with the binding free energy at the M-site, thus strengthening the protein−ligand interaction and increasing the modulation ability.

The above data strongly suggest that Pgp efflux modulation can be achieved through direct competition with molecules at SBSs, by conformational impairment at the M-site or both. As already seen for ritonavir and amprenavir, a more detailed analysis of the QZ59 isomers and tariquidar docking can shed an additional clarification on this issue. While QZ59-RRR only docks at the H-site and the M-site with a relatively high binding energy (−7.9 and −7.5 kcal·mol^{-1} respectively), QZ59-SSS is found at both SBSs and the M-site (ΔG ranging from −8.4 kcal·mol^{-1} at the M-site to −8.7 kcal·mol^{-1} at the R-site). Although the QZ59-SSS modulation capability could be explained by a high M-site cross interaction capability, a more thorough analysis of QZ59-SSS top-ranked binding pose at the R-site (Figure 6) showed a strong interaction with Ser989. The serine oxygen sits at the center of the macrocycle ring, establishing CH-π interactions with each of the three five-membered rings and allowing hydrogen-bonds between the hydroxyl group and the aromatic nitrogens. This suggests that QZ59-SSS can be firmly anchored to this point, restraining the access to the R-site, thus suppressing efflux from Pgp. QZ59-RRR, however, cannot fit in this particular region, thus not being able to impair access to the R-site. The same happens with tariquidar. This molecule also docked in all three sites with one of the lowest binding energies within this study (−10.6 kcal·mol^{-1} for M- and R-sites and −10.1 kcal·mol^{-1} for the H-site). In addition, it also seems capable of establishing strong cross interactions between both halves at the M-site. Therefore, and based on the lowest IC50 experimental value (20−145 nM),[99,100] its plausible that tariquidar can impair Pgp efflux

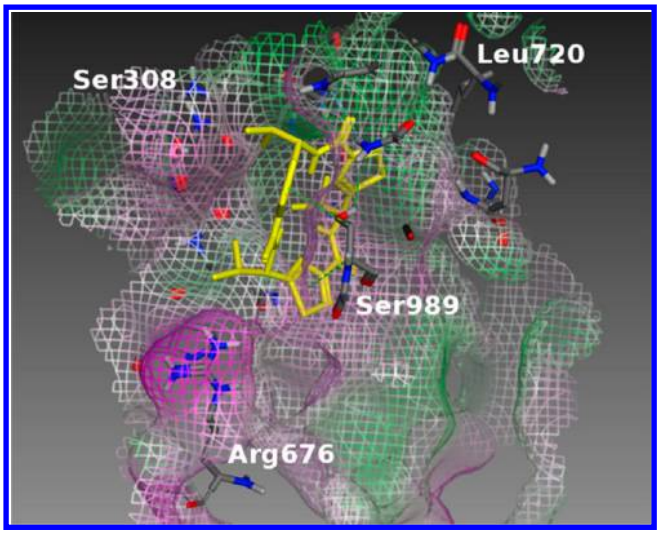

Figure 6. QZ59-SSS top-ranked binding pose (yellow) within the R-site entrance.

through the blockage of both translocation pathways (direct competition) but also by Pgp conformational alterations due to ATP binding and hydrolysis.

Probes. Molecules frequently used as efflux probes were also tested, namely digoxin, rhodamine-123, and calcein-AM. For digoxin (−10.9 kcal·mol^{-1}) and rhodamine-123 (−9.2 kcal·mol^{-1}), the calculated binding energies are identical for M- and R-sites, being the main difference the cross interaction capability, stronger in digoxin than rhodamine-123. For calcein-AM, the ΔG of M- and H-sites is also similar (−8.0 and −7.9 kcal·mol^{-1}), but a strong cross interaction capability gives to this molecule some degree of efflux modulation capability. As these molecules are used to determine Pgp efflux, it was expected that they should be found with lower binding energies at substrate-binding sites. However, several experimental studies demonstrated some degree of efflux modulation by digoxin or its metabolites[87,101] or competition between digoxin and verapamil for drug-binding sites.[102,103] For rhodamine derivatives, an inhibitory potential was also demonstrated.[104] Hence, we additionally docked the most common digoxin metabolites (digoxigenin, bis- and monodigitoxoside), rhodamine derivatives with inhibitory potency, and the hydrolyzed metabolite from calcein-AM,[105] in order to clarify the effect of these molecules on Pgp.

The results obtained were quite surprising. For digoxin metabolites, while digoxigenin was still found at both sites the bis- and monodigitoxosides docked exclusively at the R-site, with binding energies of −11.5 and −10.2 kcal·mol^{-1}, respectively (*transported substrates*— class B). In addition, the cross interaction ability of digoxigenin at the M-site it is lower than digoxin, in accordance with the experimental findings by Melchior et al.[87] For calcein, the top-ranked binding pose was found not in the H-site as calcein-AM but at the R-site with −8.5 kcal·mol^{-1}. Similarly to digoxin metabolites, the best ranked calcein docking pose found at the M-site also displayed a reduced cross interaction ability regarding calcein-AM thus, a worst modulator. As this molecule is ionized at physiological pH, lipid partitioning and the access to Pgp's internal DBP becomes severely impaired. However, it is not to be excluded some degree of efflux by Pgp at high concentrations. For rhodamine, and according to experimental results by Gannon et al.,[104] we found that the substitution of the heteroatom in the

dx.doi.org/10.1021/ci400195v | J. Chem. Inf. Model. 2013, 53, 1747−1760

xanthylium core by a sulfur (1-S) decreases the binding energy at the R-site in a larger extent than the M-site (1.0 against 0.2 kcal·mol^{-1}, respectively) and increases the cross interaction capability into a characteristic modulator (class D). When two additional rhodamine derivatives were docked (2-S and 31-S), the binding energies were lower than rhodamine-123 and the cross interaction capability at the M-site further increased. These findings are of great importance since they highlight the necessity for an adequate selection of probe substrates for Pgp efflux assays and uphold many interesting questions about the influence of probe metabolites in Pgp efflux assays.

Lipids. Several lipid molecules were also tested in order to assess the ability of Pgp as a lipid flippase (suggested in several studies[11,20,106]). However, none of the tested molecules could be classified as a Pgp substrate, all with binding energies higher than −7.0 kcal·mol^{-1}. Only cholesterol displayed binding energies similar to rhodamine-123 (−9.5 kcal·mol^{-1} for the R-site), therefore identified as a substrate.[107]

CONCLUSIONS

Although Pgp is known for many years, the full characterization of this transporter was unsuccessful, mainly due to the polyspecificity of the transported molecules and the lack of crystallographic information for more detailed studies relating structure and activity.

Several docking experiments have been performed using the murine crystallographic structure. However, the absence of the linker between both halves impaired the definition of the lower boundary of the drug-binding pocket, not allowing the determination of the substrate-binding sites location. Therefore, a refined structure based on the murine crystallographic data and obtained by means of molecular dynamics simulations[40] can be a more suitable model for docking studies due to the introduction of the missing linker sequence and equilibration within a lipid membrane.

In this study, in addition to the site determined by Aller et al., two additional drug-binding sites were identified. These sites, hereby characterized for the first time, were assigned as substrate-binding H- and R-sites, identified by Shapiro and Ling,[14] based on the docking poses of verapamil, rhodamine-123, and Hoechst 33342 and supported by experimental results (locating them near the inner leaflet interface). Therefore, the introduction of the linker sequence between both halves was essential for a correct definition of the lower boundary of the internal DBP, thus providing a clearer picture about the location of these two sites. A third site with modulatory characteristics, already described by Aller et al.,[31] was also mapped at the top of the drug-binding pocket, next to the outer leaflet of the lipid bilayer— M-site.

The assignment of the above substrate-binding sites was assessed through docking of additional molecules such as LDS-751 and anthracyclines (R-site), quercetin and colchicine (H-site), or actinomycin D, vinblastine and etoposide (for both). The results not only corroborated the previous assignment but also pointed to another interesting fact. Shapiro and Ling frequently report quercetin and colchicine as H-site substrates,[14,64] but other experimental studies by Loo and Clarke clearly locate them at the R-site.[62,63] Therefore, our results are in accordance with Loo and Clarke experimental findings but also seem to support the Didziapetris et al. minipharmacokinetic model, claiming that the combined properties of small molecules such as rhodamine-123, colchicine, or quercetin may have a positive effect on molecules efflux (also proposed by Sharom et al.).[20,67] Based on this model, quercetin and colchicine when in the presence of rhodamine-123 are able to stimulate the R-site translocation pathway (negatively affecting the H-pathway) with the magnitude of this stimulation proportional to the lipid partition of each molecule. In addition, as quercetin quenches Hoechst 33342 within the lipid bilayer, Hoechst 33342 efflux impairment will be larger when compared with the colchicine effect, as observed by Shapiro and Ling.[14]

From docking studies, it was possible to identify the lining residues for each site and, consequently, to assess several characteristics as volume, mean polarity, and residues distribution. The M-site is the most hydrophobic one, with an increased percentage of aromatic residues contributing to a relative polarity lower than the H-site and the R-site. The M-site has also the smallest volume, 30 to 39% lower than the R-site and the H-site, respectively. The H-site is the only one directly accessible from the lipid bilayer (through TMD10/12), and several linker residues were found to be common to both substrate binding sites, thus showing the importance that this structure plays in molecule recognition.

The top-ranked docking poses also allowed the identification of common features that may explain how several molecules modulate Pgp efflux. A new classification scheme was developed, in which the cross interaction capability shown by several molecules at the M-site is a key feature to distinguish substrates from modulators. The properties of the most common efflux probes and their metabolites were also assessed, being identified some modulatory characteristics in several of the evaluated molecules which has implications in the interpretation of the different efflux assay results. Lipid molecules were also evaluated, but the binding energy registered for these molecules classifies them as Pgp non-substrates. Due to a relatively high standard error associated with docking techniques (2.85 kcal·mol^{-1} for VINA[48]), 35% of the molecules could not be classified as substrates or modulators. However, the modulation capability of these molecules can be inferred by low binding energies in conjunction with the cross interaction capability displayed at the M-site, as demonstrated for QZ59-SSS and tariquidar. The cross interaction capability offers, for the first time, a suitable explanation for the modulation capability associated with molecules frequently classified as substrates, as indinavir (IC_{50} of 17−44 μM),[85,97] ritonavir (IC_{50} of 1.29 μM),[97] reserpine (IC_{50} of 4.0−10 μM),[7,77] colchicine (IC_{50} of 89−230 μM),[85−87] or vinblastine (IC_{50} of 18−90 μM).[43,74]

Despite the results above-described, there is sufficient experimental information needing clarification that clearly shows that Pgp efflux mechanism is far from being understood. Several studies pointed out that Pgp and the surrounding lipid bilayer act as one functional unit,[108,109] with lipid composition[110−112] and molecules global permeation rate through the membrane[113,114] being as important as the transporter itself. In addition, little is known about diffusion of molecules from the bilayer toward the Pgp internal drug-binding pocket, being of great relevance additional studies on this process.

However, we can only speculate if the R-site/H-site assignment is maintained during the full efflux cycle. When taking into account the alternate model[68] (in which ATP hydrolysis occurs alternately in NBD1 and NBD2), the substrate-binding sites may present different characteristics at different steps of the efflux mechanism, possibly interconverting the H-site and the R-site in one another, partially explaining the induced-fit and polyspecificity models proposed for Pgp

substrate recognition. Still, a comprehensive study of the full dynamic efflux cycle is out of reach in the time scale of atomistic molecular dynamics simulations.

With the present work, we aim to make a contribution that, hopefully, will stimulate the development of new experimental studies, in order to thoroughly characterize the substrate-binding sites properties and, in the end, allowing the development of more potent and selective Pgp efflux modulators.

■ ASSOCIATED CONTENT

Supporting Information

Tables containing the molecules included in each set and their classification according the multistep classification algorithm (Tables S1−S4) and a spreadsheet with LigPlot interactions output (Tables S5 and S6). This material is available free of charge via the Internet at http://pubs.acs.org.

■ AUTHOR INFORMATION

Corresponding Author

*E-mail: dsantos@ff.ul.pt. Corresponding author address: Research Institute for Medicines and Pharmaceutical Sciences (iMed.UL), Faculty of Pharmacy, University of Lisbon, Av. Prof. Gama Pinto, 1649-003 Lisbon, Portugal.

Author Contributions

These authors contributed equally.

Notes

The authors declare no competing financial interest.

■ ACKNOWLEDGMENTS

This work was supported by *Fundação para a Ciência e Tecnologia, I.P.* (FCT, Portugal) through projects PTDC/QUI-QUI/099815/2008, Pest-OE/SAU/UI4013/2011, and PTDC/QEQ-MED/0905/2012. Ricardo Ferreira acknowledges FCT for the PhD grant SFRH/BD/84285/2012.

■ REFERENCES

(1) Locher, K. P. Structure and mechanism of ATP-binding cassette transporters. *Philos. Trans. R. Soc. London, Ser. B* **2009**, *364*, 239−245.

(2) Tsuruo, T.; Lida, H.; Tsukagoshi, S.; Sakurai, Y. Overcoming of vincristine resistance in P388 leukemia in vivo and in vitro through enhanced cytotoxicity of vincristine and vinblastine by verapamil. *Cancer Res.* **1981**, *41*, 1967−1972.

(3) Ford, J. M.; Prozialeck, W. C.; Hait, W. N. Structural features determining activity of phenothiazines and related drugs for inhibition of cell growth and reversal of multidrug resistance. *Mol. Pharmacol.* **1989**, *35*, 105−115.

(4) Reis, M. A.; Ferreira, R. J.; Santos, M. M. M.; dos Santos, D. J. V. A.; Molnár, J.; Ferreira, M. J. U. Enhancing macrocyclic diterpenes as multidrug-resistance reversers: structure-activity studies on jolkinol D derivatives. *J. Med. Chem.* **2013**, *56*, 748−760.

(5) Seelig, A. How does P-glycoprotein recognize its substrates? *Int. J. Clin. Pharmacol. Ther.* **1998**, *36*, 50−54.

(6) Suzuki, T.; Fukazawa, N.; San-nohe, K. Structure-activity relationship of newly synthesized quinoline derivatives for reversal of multidrug resistance in cancer. *J. Med. Chem.* **1997**, *40*, 2047−2052.

(7) Pearce, H. L.; Safa, A. R.; Bach, N. J.; Winter, M. A.; Cirtain, M. C.; Beck, W. T. Essential features of the P-glycoprotein pharmacophore as defined by a series of reserpine analogs that modulate multidrug resistance. *Proc. Natl. Acad. Sci. U. S. A.* **1989**, *86*, 5128−5132.

(8) Ferreira, R. J.; dos Santos, D. J. V. A.; Ferreira, M.-J. U.; Guedes, R. C. Toward a better pharmacophore description of P-glycoprotein modulators, based on macrocyclic diterpenes from Euphorbia species. *J. Chem. Inf. Model.* **2011**, *51*, 1315−1324.

(9) Pajeva, I. K.; Wiese, M. Pharmacophore model of drugs involved in P-glycoprotein multidrug resistance: explanation of structural variety (hypothesis). *J. Med. Chem.* **2002**, *45*, 5671−5686.

(10) Pajeva, I. K.; Globisch, C.; Wiese, M. Combined pharmacophore modeling, docking, and 3D QSAR studies of ABCB1 and ABCC1 transporter inhibitors. *ChemMedChem* **2009**, *4*, 1883−1896.

(11) Higgins, C. F.; Gottesman, M. M. Is the multidrug transporter a flippase? *Trends Biochem. Sci.* **1992**, *17*, 18−21.

(12) Altenberg, G. A.; Vanoye, C. G.; Horton, J. K.; Reuss, L.; Julie, K. Unidirectional fluxes of rhodamine 123 in multidrug-resistant cells: evidence against direct drug extrusion from the plasma membrane. *Proc. Natl. Acad. Sci. U. S. A.* **1994**, *91*, 4654−4657.

(13) Raviv, Y.; Pollard, H. B.; Bruggemann, E. P.; Pastan, I.; Gottesman, M. M. Photosensitized labeling of a functional multidrug transporter in living drug-resistant tumor cells. *J. Biol. Chem.* **1990**, *265*, 3975−3980.

(14) Shapiro, A. B.; Ling, V. Positively cooperative sites for drug transport by P-glycoprotein with distinct drug specificities. *Eur. J. Biochem.* **1997**, *250*, 130−137.

(15) Shapiro, A. B.; Ling, V. Transport of LDS-751 from the cytoplasmic leaflet of the plasma membrane by the rhodamine-123-selective site of P-glycoprotein. *Eur. J. Biochem.* **1998**, *254*, 181−188.

(16) Parveen, Z.; Stockner, T.; Bentele, C.; Pferschy, S.; Kraupp, M.; Freissmuth, M.; Ecker, G. F.; Chiba, P. Molecular dissection of dual pseudosymmetric solute translocation pathways in human P-glycoprotein. *Mol. Pharmacol.* **2011**, *79*, 443−452.

(17) Pleban, K.; Kopp, S.; Csaszar, E.; Peer, M.; Hrebicek, T.; Rizzi, A.; Ecker, G. F.; Chiba, P. P-glycoprotein substrate binding domains are located at the transmembrane domain/transmembrane domain interfaces: a combined photoaffinity labeling-protein homology modeling approach. *Mol. Pharmacol.* **2005**, *67*, 365−374.

(18) Loo, T. W.; Clarke, D. M. Recent progress in understanding the mechanism of P-glycoprotein-mediated drug efflux. *J. Membr. Biol.* **2005**, *206*, 173−185.

(19) Shapiro, A. B.; Fox, K.; Lam, P.; Ling, V. Stimulation of P-glycoprotein-mediated drug transport by prazosin and progesterone. *Eur. J. Biochem.* **2001**, *259*, 841−850.

(20) Sharom, F. J.; Lugo, M. R.; Eckford, P. D. W. New insights into the drug binding, transport and lipid flippase activities of the p-glycoprotein multidrug transporter. *J. Bioenerg. Biomembr.* **2005**, *37*, 481−487.

(21) Lugo, M. R.; Sharom, F. J. Interaction of LDS-751 with P-glycoprotein and mapping of the location of the R drug binding site. *Biochemistry* **2005**, *44*, 643−655.

(22) Loo, T. W.; Bartlett, M. C.; Clarke, D. M. Simultaneous binding of two different drugs in the binding pocket of the human multidrug resistance P-glycoprotein. *J. Biol. Chem.* **2003**, *278*, 39706−39710.

(23) Loo, T. W.; Clarke, D. M. Do drug substrates enter the common drug-binding pocket of P-glycoprotein through "gates"? *Biochem. Biophys. Res. Commun.* **2005**, *329*, 419−422.

(24) Loo, T. W.; Clarke, D. M. Determining the dimensions of the drug-binding domain of human P-glycoprotein using thiol cross-linking compounds as molecular rulers. *J. Biol. Chem.* **2001**, *276*, 36877−36880.

(25) Mandal, D.; Moitra, K.; Ghosh, D.; Xia, D.; Dey, S. Evidence for modulatory sites at the lipid-protein interface of the human multidrug transporter p-glycoprotein. *Biochemistry* **2012**, *51*, 2852−2866.

(26) Rosenberg, M. F.; Callaghan, R.; Modok, S.; Higgins, C. F.; Ford, R. C. Three-dimensional structure of P-glycoprotein: the transmembrane regions adopt an asymmetric configuration in the nucleotide-bound state. *J. Biol. Chem.* **2005**, *280*, 2857−2862.

(27) Chang, G.; Roth, C. B. Structure of MsbA from E. coli: a homolog of the multidrug resistance ATP binding cassette (ABC) transporters. *Science* **2001**, *293*, 1793−1800.

(28) Locher, K. P.; Lee, A. T.; Rees, D. C. The E. coli BtuCD structure: a framework for ABC transporter architecture and mechanism. *Science* **2002**, *296*, 1091−1098.

(29) Loo, T. W.; Bartlett, M. C.; Clarke, D. M. Identification of residues in the drug translocation pathway of the human multidrug

resistance P-glycoprotein by arginine mutagenesis. *J. Biol. Chem.* **2009**, *284*, 24074−24087.
(30) Berman, H. M.; Westbrook, J.; Feng, Z.; Gilliland, G.; Bhat, T. N.; Weissig, H.; Shindyalov, I. N.; Bourne, P. E. The Protein Data Bank. *Nucleic Acids Res.* **2000**, *28*, 235−242.
(31) Aller, S. G.; Yu, J.; Ward, A.; Weng, Y.; Chittaboina, S.; Zhuo, R.; Harrell, P. M.; Trinh, Y. T.; Zhang, Q.; Urbatsch, I. L.; Chang, G. Structure of P-glycoprotein reveals a molecular basis for poly-specific drug binding. *Science* **2009**, *323*, 1718−1722.
(32) Jabeen, I.; Wetwitayaklung, P.; Klepsch, F.; Parveen, Z.; Chiba, P.; Ecker, G. F. Probing the stereoselectivity of P-glycoprotein-synthesis, biological activity and ligand docking studies of a set of enantiopure benzopyrano[3,4-b][1,4]oxazines. *Chem. Commun. (Cambridge, U. K.)* **2011**, *47*, 2586−2588.
(33) Ford, J. M.; Yang, J. M.; Hait, W. N. P-glycoprotein-mediated multidrug resistance: experimental and clinical strategies for its reversal. *Cancer Treat. Res.* **1996**, *87*, 3−38.
(34) Kwon, Y.; Kamath, A. V.; Morris, M. E. Inhibitors of P-glycoprotein-mediated daunomycin transport in rat liver canalicular membrane vesicles. *J. Pharm. Sci.* **1996**, *85*, 935−939.
(35) Pajeva, I. K.; Globisch, C.; Wiese, M. Structure-function relationships of multidrug resistance P-glycoprotein. *J. Biol. Chem.* **2004**, *47*, 2523−2533.
(36) Dolghih, E.; Bryant, C.; Renslo, A. R.; Jacobson, M. P. Predicting binding to P-glycoprotein by flexible receptor docking. *PLoS Comput. Biol.* **2011**, *7*, e1002083.
(37) Hrycyna, C. A.; Airan, L. E.; Germann, U. A.; Ambudkar, S. V; Pastan, I.; Gottesman, M. M. Structural flexibility of the linker region of human P-glycoprotein permits ATP hydrolysis and drug transport. *Biochemistry* **1998**, *37*, 13660−13673.
(38) Sato, T.; Kodan, A.; Kimura, Y.; Ueda, K.; Nakatsu, T.; Kato, H. Functional role of the linker region in purified human P-glycoprotein. *FEBS J.* **2009**, *276*, 3504−3516.
(39) Ferreira, R. J.; Ferreira, M.-J. U.; dos Santos, D. J. V. A. Assessing the stabilization of P-glycoprotein's nucleotide-binding domains by the linker, using molecular dynamics. *Mol. Inf.* **2013**, *32*, 529−540.
(40) Ferreira, R. J.; Ferreira, M. J. U.; dos Santos, D. J. V. A. Insights on P-glycoprotein's efflux mechanism obtained by molecular dynamics simulations. *J. Chem. Theory Comput.* **2012**, *8*, 1853−1864.
(41) Jin, M. S.; Oldham, M. L.; Zhang, Q.; Chen, J. Crystal structure of the multidrug transporter P-glycoprotein from Caenorhabditis elegans. *Nature* **2012**, *490*, 566−569.
(42) Polli, J. W.; Wring, S. A.; Humphreys, J. E.; Huang, L.; Morgan, J. B.; Webster, L. O.; Serabjit-Singh, C. S. Rational use of in vitro P-glycoprotein assays in drug discovery. *J. Pharmacol. Exp. Ther.* **2001**, *299*, 620−8.
(43) Rautio, J.; Humphreys, J. E.; Webster, L. O.; Balakrishnan, A.; Keogh, J. P.; Kunta, J. R.; Serabjit-Singh, C. J.; Polli, J. W. In vitro p-glycoprotein inhibition assays for assessment of clinical drug interaction potential of new drug candidates: a recommendation for probe substrates. *Drug Metab. Dispos.* **2006**, *34*, 786−792.
(44) MarvinSketch 5.11.1, 2012, ChemAxon. http://www.chemaxon.com (accessed June 27, 2013).
(45) *Molecular Operating Environment (MOE)*, 2010.10; Chemical Computing Group Inc., 1010 Sherbooke St. West, Suite #910, Montreal, QC, Canada, H3A 2R7, 2010.
(46) Sanner, M. F. Python: a programming language for software integration and development. *J. Mol. Graphics Modell.* **1999**, *17*, 57−61.
(47) Morris, G. M.; Huey, R.; Lindstrom, W.; Sanner, M. F.; Belew, R. K.; Goodsell, D. S.; Olson, A. J. AutoDock4 and AutoDockTools4: automated docking with selective receptor flexibility. *J. Comput. Chem.* **2009**, *30*, 2785−2791.
(48) Trott, O.; Olson, A. J. AutoDock Vina: improving the speed and accuracy of docking with a new scoring function, efficient optimization, and multithreading. *J. Comput. Chem.* **2010**, *31*, 455−461.
(49) Brady, G. P.; Stouten, P. F. Fast prediction and visualization of protein binding pockets with PASS. *J. Comput.-Aided Mol. Des.* **2000**, *14*, 383−401.
(50) Kohlbacher, O.; Lenhof, H. P. BALL–rapid software prototyping in computational molecular biology. Biochemicals Algorithms Library. *Bioinformatics* **2000**, *16*, 815−824.
(51) Eyrisch, S.; Helms, V. Transient pockets on protein surfaces involved in protein-protein interaction. *J. Med. Chem.* **2007**, *50*, 3457−64.
(52) Wallace, A. C.; Laskowski, R. A.; Thornton, J. M. LIGPLOT: a program to generate schematic diagrams of protein-ligand interactions. *Protein Eng.* **1995**, *8*, 127−134.
(53) McDonald, I. K.; Thornton, J. M. Satisfying hydrogen bonding potential in proteins. *J. Mol. Biol.* **1994**, *238*, 777−793.
(54) Wang, R. B.; Kuo, C. L.; Lien, L. L.; Lien, E. J.-C. Structure-activity relationship: analyses of p-glycoprotein substrates and inhibitors. *J. Clin. Pharm. Ther.* **2003**, *28*, 203−228.
(55) Xue, Y.; Yap, C. W.; Sun, L. Z.; Cao, Z. W.; Wang, J. F.; Chen, Y. Z. Prediction of P-glycoprotein substrates by a support vector machine approach. *J. Chem. Inf. Comput. Sci.* **2004**, *44*, 1497−1505.
(56) Cabrera, M. A.; González, I.; Fernández, C.; Navarro, C.; Bermejo, M. A topological substructural approach for the prediction of P-glycoprotein substrates. *J. Pharm. Sci.* **2006**, *95*, 589−606.
(57) Wiese, M.; Pajeva, I. K. Structure-activity relationships of multidrug resistance reversers. *Curr. Med. Chem.* **2001**, *8*, 685−713.
(58) Loo, T. W.; Clarke, D. M. Identification of residues in the drug-binding domain of human P-glycoprotein. Analysis of transmembrane segment 11 by cysteine-scanning mutagenesis and inhibition by dibromobimane. *J. Biol. Chem.* **1999**, *274*, 35388−35392.
(59) Loo, T. W.; Clarke, D. M. Defining the drug-binding site in the human multidrug resistance P-glycoprotein using a methanethiosulfonate analog of verapamil, MTS-verapamil. *J. Biol. Chem.* **2001**, *276*, 14972−14979.
(60) Loo, T. W.; Clarke, D. M. Location of the rhodamine-binding site in the human multidrug resistance P-glycoprotein. *J. Biol. Chem.* **2002**, *277*, 44332−44338.
(61) Qu, Q.; Sharom, F. J. Proximity of bound Hoechst 33342 to the ATPase catalytic sites places the drug binding site of P-glycoprotein within the cytoplasmic membrane leaflet. *Biochemistry* **2002**, *41*, 4744−4752.
(62) Loo, T. W.; Clarke, D. M. Identification of residues within the drug-binding domain of the human multidrug resistance P-glycoprotein by cysteine-scanning mutagenesis and reaction with dibromobimane. *J. Biol. Chem.* **2000**, *275*, 39272−39278.
(63) Loo, T. W. Identification of residues in the drug-binding site of human P-glycoprotein Using a Thiol-reactive Substrate. *J. Biol. Chem.* **1997**, *272*, 31945−31948.
(64) Shapiro, A. B.; Ling, V. Effect of quercetin on Hoechst 33342 transport by purified and reconstituted P-glycoprotein. *Biochem. Pharmacol.* **1997**, *53*, 587−596.
(65) Safa, A. R.; Glover, C. J.; Sewell, J. L.; Meyers, M. B.; Biedler, J. L.; Felsted, R. L. Identification of the multidrug resistance-related membrane glycoprotein as an acceptor for calcium channel blockers. *J. Biol. Chem.* **1987**, *262*, 7884−7888.
(66) Tamai, I.; Safa, A. R. Azidopine noncompetitively interacts with vinblastine and cyclosporin A binding to P-glycoprotein in multidrug resistant cells. *J. Biol. Chem.* **1991**, *266*, 16796−16800.
(67) Didziapetris, R.; Japertas, P.; Avdeef, A.; Petrauskas, A. Classification analysis of P-glycoprotein substrate specificity. *J. Drug Targeting* **2003**, *11*, 391−406.
(68) Senior, A. E.; Al-Shawi, M. K.; Urbatsch, I. L. The catalytic cycle of P-glycoprotein. *FEBS Lett.* **1995**, *377*, 285−289.
(69) Martin, C.; Berridge, G.; Mistry, P.; Higgins, C.; Charlton, P.; Callaghan, R. Drug binding sites on P-glycoprotein are altered by ATP binding prior to nucleotide hydrolysis. *Biochemistry* **2000**, *39*, 11901−11906.
(70) Callaghan, R.; Ford, R. C.; Kerr, I. D. The translocation mechanism of P-glycoprotein. *FEBS Lett.* **2006**, *580*, 1056−1063.

(71) Siarheyeva, A.; Liu, R.; Sharom, F. J. Characterization of an asymmetric occluded state of P-glycoprotein with two bound nucleotides: implications for catalysis. *J. Biol. Chem.* **2010**, *285*, 7575−7586.
(72) Reis, M.; Ferreira, R. J.; Serly, J.; Duarte, N.; Madureira, A. M.; dos Santos, D. J. V. A.; Molnar, J.; Ferreira, M.-J. U. Colon adenocarcinoma multidrug resistance reverted by euphorbia diterpenes: structure-activity relationships and pharmacophore modeling. *Anticancer Agents Med. Chem.* **2012**, *12*, 1015−1024.
(73) Gutmann, D. A. P.; Ward, A.; Urbatsch, I. L.; Chang, G.; Van Veen, H. W. Understanding polyspecificity of multidrug ABC transporters: closing in on the gaps in ABCB1. *Trends Biochem. Sci.* **2010**, *35*, 36−42.
(74) Wang, E.; Casciano, C. N.; Clement, R. P.; Johnson, W. W. The farnesyl protein transferase inhibitor SCH66336 is a potent inhibitor of MDR1 product P-glycoprotein. *Cancer Res.* **2001**, *61*, 7525−7529.
(75) Chen, C.; Hanson, E.; Watson, J. W.; Lee, J. S. P-glycoprotein limits the brain penetration of nonsedating but not sedating H1-antagonists. *Drug Metab. Dispos.* **2003**, *31*, 312−318.
(76) Romiti, N.; Tramonti, G.; Chieli, E. Influence of different chemicals on MDR-1 P-glycoprotein expression and activity in the HK-2 proximal tubular cell line. *Toxicol. Appl. Pharmacol.* **2002**, *183*, 83−91.
(77) Akiyama, S.; Cornwell, M. M.; Kuwano, M.; Pastan, I.; Gottesman, M. M. Most drugs that reverse multidrug resistance also inhibit photoaffinity labeling of P-glycoprotein by a vinblastine analog. *Mol. Pharmacol.* **1988**, *33*, 144−147.
(78) Vezmar, M.; Georges, E. Direct binding of chloroquine to the multidrug resistance protein (MRP): possible role for MRP in chloroquine drug transport and resistance in tumor cells. *Biochem. Pharmacol.* **1998**, *56*, 733−742.
(79) De Graaf, D.; Sharma, R. C.; Mechetner, E. B.; Schimke, R. T.; Roninson, I. B. P-glycoprotein confers methotrexate resistance in 3T6 cells with deficient carrier-mediated methotrexate uptake. *Proc. Natl. Acad. Sci. U. S. A.* **1996**, *93*, 1238−1242.
(80) Norris, M. D.; De Graaf, D.; Haber, M.; Kavallaris, M.; Madafiglio, J.; Gilbert, J.; Kwan, E.; Stewart, B. W.; Mechetner, E. B.; Gudkov, A. V; Roninson, I. B. Involvement of MDR1 P-glycoprotein in multifactorial resistance to methotrexate. *Int. J. Cancer* **1996**, *65*, 613−619.
(81) Gifford, A. J.; Kavallaris, M.; Madafiglio, J.; Matherly, L. H.; Stewart, B. W.; Haber, M.; Norris, M. D. P-glycoprotein-mediated methotrexate resistance in CCRF-CEM sublines deficient in methotrexate accumulation due to a point mutation in the reduced folate carrier gene. *Int. J. Cancer* **1998**, *78*, 176−181.
(82) Riffkin, C. D.; Chung, R.; Wall, D. M.; Zalcberg, J. R.; Cowman, A. F.; Foley, M.; Tilley, L. Modulation of the function of human MDR1 P-glycoprotein by the antimalarial drug mefloquine. *Biochem. Pharmacol.* **1996**, *52*, 1545−1552.
(83) Pham, Y. T.; Régina, A.; Farinotti, R.; Couraud, P.; Wainer, I. W.; Roux, F.; Gimenez, F. Interactions of racemic mefloquine and its enantiomers with P-glycoprotein in an immortalised rat brain capillary endothelial cell line, GPNT. *Biochim. Biophys. Acta* **2000**, *1524*, 212−219.
(84) Ford, J. M.; Bruggemann, E. P.; Pastan, I.; Gottesman, M. M.; Hait, W. N. Cellular and biochemical characterization of thioxanthenes for reversal of multidrug resistance in human and murine cell lines. *Cancer Res.* **1990**, *50*, 1748−1756.
(85) Ekins, S.; Kim, R. B.; Leake, B. F.; Dantzig, A. H.; Schuetz, E. G.; Lan, L.-B.; Yasuda, K.; Shepard, R. L.; Winter, M. A.; Schuetz, J. D.; Wikel, J. H.; Wrighton, S. A. Application of three-dimensional quantitative structure-activity relationships of P-glycoprotein inhibitors and substrates. *Mol. Pharmacol.* **2002**, *61*, 974−981.
(86) Ekins, S.; Kim, R. B.; Leake, B. F.; Dantzig, A. H.; Schuetz, E. G.; Lan, L.-B.; Yasuda, K.; Shepard, R. L.; Winter, M. A.; Schuetz, J. D.; Wikel, J. H.; Wrighton, S. A. Three-dimensional quantitative structure-activity relationships of inhibitors of P-glycoprotein. *Mol. Pharmacol.* **2002**, *61*, 964−973.
(87) Melchior, D. L.; Sharom, F. J.; Evers, R.; Wright, G. E.; Chu, J. W. K.; Wright, S. E.; Chu, X.; Yabut, J. Determining P-glycoprotein-drug interactions: evaluation of reconstituted P-glycoprotein in a liposomal system and LLC-MDR1 polarized cell monolayers. *J. Pharmacol. Toxicol. Methods* **2012**, *65*, 64−74.
(88) Wang, E. J.; Lew, K.; Casciano, C. N.; Clement, R. P.; Johnson, W. W. Interaction of common azole antifungals with P glycoprotein. *Antimicrob. Agents Chemother.* **2002**, *46*, 160−165.
(89) Kurosawa, M.; Okabe, M.; Hara, N.; Kawamura, K.; Suzuki, S.; Sakurada, K.; Asaka, M. Reversal effect of itraconazole on adriamycin and etoposide resistance in human leukemia cells. *Ann. Hematol.* **1996**, *72*, 17−21.
(90) Van Zuylen, L.; Sparreboom, A.; Van der Gaast, A.; Van der Burg, M. E.; Van Beurden, V.; Bol, C. J.; Woestenborghs, R.; Palmer, P. A.; Verweij, J. The orally administered P-glycoprotein inhibitor R101933 does not alter the plasma pharmacokinetics of docetaxel. *Clin. Cancer Res.* **2000**, *6*, 1365−1371.
(91) Van Zuylen, L.; Sparreboom, A.; Van der Gaast, A.; Nooter, K.; Eskens, F. A. L. M.; Brouwer, E.; Bol, C. J.; De Vries, R.; Palmer, P. A.; Verweij, J. Disposition of docetaxel in the presence of P-glycoprotein inhibition by intravenous administration of R101933. *Eur. J. Cancer* **2002**, *38*, 1090−1099.
(92) Duarte, N.; Varga, A.; Cherepnev, G.; Radics, R.; Molnár, J.; Ferreira, M.-J. U. Apoptosis induction and modulation of P-glycoprotein mediated multidrug resistance by new macrocyclic lathyrane-type diterpenoids. *Bioorg. Med. Chem.* **2007**, *15*, 546−554.
(93) Dantzig, A. H.; Shepard, R. L.; Cao, J.; Law, K. L.; Ehlhardt, W. J.; Baughman, T. M.; Bumol, T. F.; Starling, J. J. Reversal of P-glycoprotein-mediated multidrug resistance by a potent cyclopropyldibenzosuberane modulator, LY335979. *Cancer Res.* **1996**, *56*, 4171−4179.
(94) Kondratov, R. V; Komarov, P. G.; Becker, Y.; Ewenson, A.; Gudkov, A. V Small molecules that dramatically alter multidrug resistance phenotype by modulating the substrate specificity of P-glycoprotein. *Proc. Natl. Acad. Sci. U. S. A.* **2001**, *98*, 14078−14083.
(95) Störmer, E.; Perloff, M. D.; Von Moltke, L. L.; Greenblatt, D. J. Methadone inhibits rhodamine123 transport in Caco-2 cells. *Drug Metab. Dispos.* **2001**, *29*, 954−956.
(96) Brooks, T. A.; Minderman, H.; O'Loughlin, K. L.; Pera, P.; Ojima, I.; Baer, M. R.; Bernacki, R. J.; Brooks, T. Taxane-based reversal agents modulate drug resistance mediated by P-glycoprotein, multidrug resistance protein, and breast cancer resistance protein. *Mol. Cancer Ther.* **2003**, *2*, 1195−205.
(97) Storch, C. H.; Theile, D.; Lindenmaier, H.; Haefeli, W. E.; Weiss, J. Comparison of the inhibitory activity of anti-HIV drugs on P-glycoprotein. *Biochem. Pharmacol.* **2007**, *73*, 1573−1581.
(98) Zha, W.; Wang, G.; Xu, W.; Liu, X.; Wang, Y.; Zha, B. S.; Shi, J.; Zhao, Q.; Gerk, P. M.; Studer, E.; Hylemon, P. B.; Pandak, W. M.; Zhou, H. Inhibition of P-glycoprotein by HIV protease inhibitors increases intracellular accumulation of berberine in murine and human macrophages. *PloS One* **2013**, *8*, e54349.
(99) Mistry, P.; Stewart, A. J.; Dangerfield, W.; Okiji, S.; Liddle, C.; Bootle, D.; Plumb, J. A.; Templeton, D.; Charlton, P. In vitro and in vivo reversal of P-glycoprotein-mediated multidrug resistance by a novel potent modulator, XR9576. *Cancer Res.* **2001**, *61*, 749−758.
(100) Sterz, K.; Möllmann, L.; Jacobs, A.; Baumert, D.; Wiese, M. Activators of P-glycoprotein: structure-activity relationships and investigation of their mode of action. *ChemMedChem* **2009**, *4*, 1897−1911.
(101) Gozalpour, E.; Wittgen, H. G. M.; Van den Heuvel, J. J. M. W.; Greupink, R.; Russel, F. G. M.; Koenderink, J. B. Interaction of digitalis-like compounds with p-glycoprotein. *Toxicol. Sci.* **2013**, *131*, 502−511.
(102) Funakoshi, S.; Murakami, T.; Yumoto, R.; Kiribayashi, Y.; Takano, M. Role of P-glycoprotein in pharmacokinetics and drug interactions of digoxin and beta-methyldigoxin in rats. *J. Pharm. Sci.* **2003**, *92*, 1455−1463.

(103) Rebbeor, J. F.; Senior, A. E. Effects of cardiovascular drugs on ATPase activity of P-glycoprotein in plasma membranes and in purified reconstituted form. *Biochim. Biophys. Acta* **1998**, *1369*, 85−93.
(104) Gannon, M. K.; Holt, J. J.; Bennett, S. M.; Wetzel, B. R.; Loo, T. W.; Bartlett, M. C.; Clarke, D. M.; Sawada, G. A.; Higgins, J. W.; Tombline, G.; Raub, T. J.; Detty, M. R. Rhodamine inhibitors of P-glycoprotein: an amide/thioamide "switch" for ATPase activity. *J. Med. Chem.* **2009**, *52*, 3328−3341.
(105) Tenopoulou, M.; Kurz, T.; Doulias, P.-T.; Galaris, D.; Brunk, U. T. Does the calcein-AM method assay the total cellular "labile iron pool" or only a fraction of it? *Biochem. J.* **2007**, *403*, 261−266.
(106) Eckford, P. D. W.; Sharom, F. J. The reconstituted P-glycoprotein multidrug transporter is a flippase for glucosylceramide and other simple glycosphingolipids. *Biochem. J.* **2005**, *389*, 517−526.
(107) Garrigues, A.; Escargueil, A. E.; Orlowski, S. The multidrug transporter, P-glycoprotein, actively mediates cholesterol redistribution in the cell membrane. *Proc. Natl. Acad. Sci. U. S. A.* **2002**, *99*, 10347−10352.
(108) Lee, A. G. Lipid−protein interactions in biological membranes: a structural perspective. *Biochim. Biophys. Acta* **2003**, *1612*, 1−40.
(109) Klappe, K.; Hummel, I.; Hoekstra, D.; Kok, J. W. Lipid dependence of ABC transporter localization and function. *Chem. Phys. Lipids* **2009**, *161*, 57−64.
(110) Eytan, G. D.; Regev, R.; Oren, G.; Assaraf, Y. G. The role of passive transbilayer drug movement in multidrug resistance and its modulation. *J. Biol. Chem.* **1996**, *271*, 12897−12902.
(111) Urbatsch, I. L.; Senior, A. E. Effects of lipids on ATPase activity of purified Chinese hamster P-glycoprotein. *Arch. Biochem. Biophys.* **1995**, *316*, 135−40.
(112) Orlowski, S.; Martin, S.; Escargueil, A. P-glycoprotein and "lipid rafts": some ambiguous mutual relationships (floating on them, building them or meeting them by chance?). *Cell. Mol. Life Sci.* **2006**, *63*, 1038−1059.
(113) Eytan, G. D.; Kuchel, P. W. Mechanism of action of P-glycoprotein in relation to passive membrane permeation. *Int. Rev. Cytol.* **1999**, *190*, 175−250.
(114) Regev, R.; Katzir, H.; Yeheskely-Hayon, D.; Eytan, G. D. Modulation of P-glycoprotein-mediated multidrug resistance by acceleration of passive drug permeation across the plasma membrane. *FEBS Lett.* **2007**, *274*, 6204−6214.